Electronic Supplementary Material (ESI) for Journal of Materials Chemistry C.

Supporting Information for:

Nanofibers generated from linear carbazole-based organogelators for the detection of explosives

Guanghui Hong, Jingbo Sun, Chong Qian, Pengchong Xue, Peng Gong, Zhenqi Zhang, Ran Lu*

State Key Laboratory of Supramolecular Structure and Materials, College of Chemistry, Jilin University, Changchun 130012, P. R. China

Fax: +86-431-88923907; Tel: +86-431-88499179

E-Mail: luran@mail.jlu.edu.cn

Table S1. Photophysical and electrochemical data of **C3** and **C5**.

Compounds	Solutions[a]			Nanofiber films		E_{onset}^{ox}	HOMO	LUMO
	λ^{abs}_{max} (nm)	λ^{em}_{max} (nm)	Φ_F[b]	λ^{abs}_{max} (nm)	λ^{em}_{max} (nm)	(eV)[c]	(eV)[d]	(eV)[e]
TC3T	258, 330, 376	427, 449	0.380	339, 385, 413	456, 483	0.35	-4.83	-1.93
PC3P	267, 332, 371	488	0.256	274, 333, 383	479	0.26	-4.74	-1.86

[a] In CH_2Cl_2 (1μM).

[b] Using quinine sulfate in 0.1 H_2SO_4 (Φ_F = 0.546) as the standard.

[c] Using E^{ox}_{onset} is the onset oxidation potential.

[d] Using HOMO = $-(E^{ox}_{onset} + 4.48)$ eV.

[e] LUMO=HOMO−Eg, Eg is determined from the onset of the absorption at the lower energy band edge.

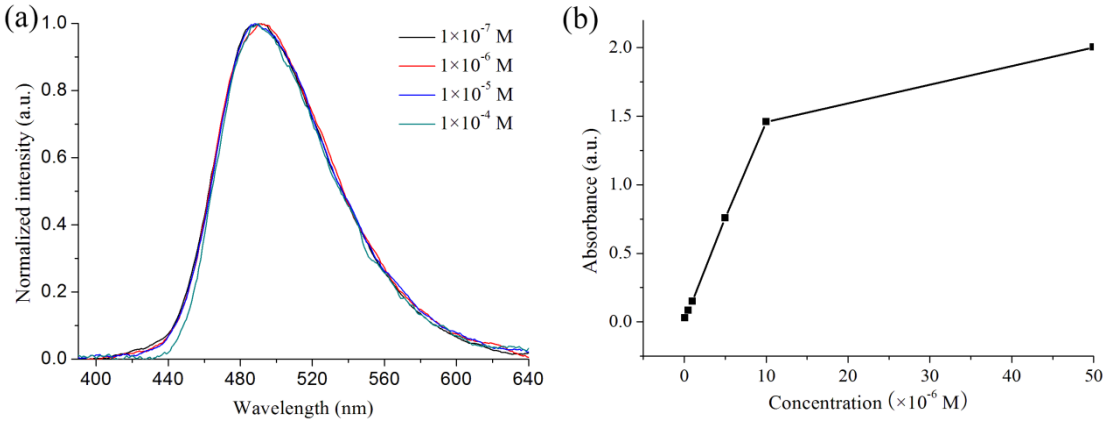

Figure S1 (a) Normalized concentration-dependent fluorescence emission spectra of **PC3P** in CH_2Cl_2 (λ_{ex} = 376 nm) and (b) The plot of the absorbance at 326 nm *vers* the concentration of **PC3P** in CH_2Cl_2.

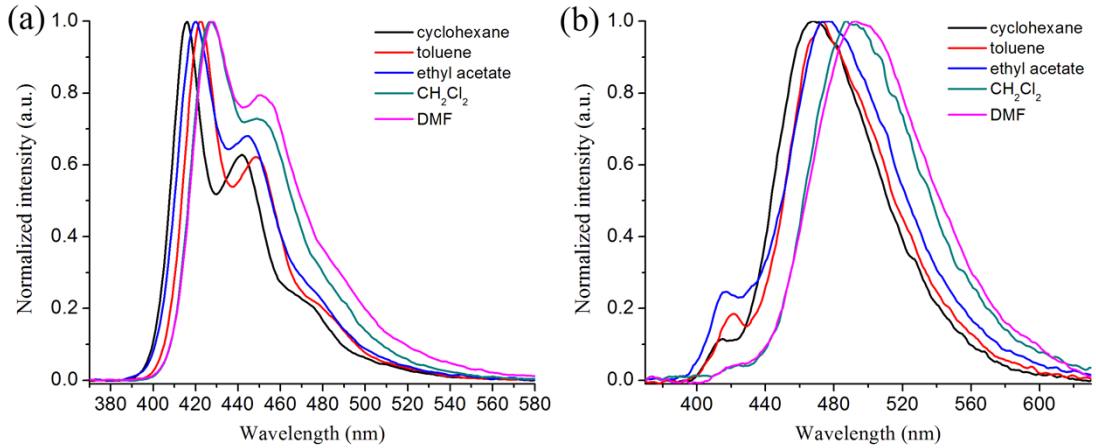

Figure S2 Normalized fluorescence emission spectra of **TC3T** (a) and **PC3P** (b) in different solvents (1.0×10^{-6} M), λ_{ex} = 376 nm.

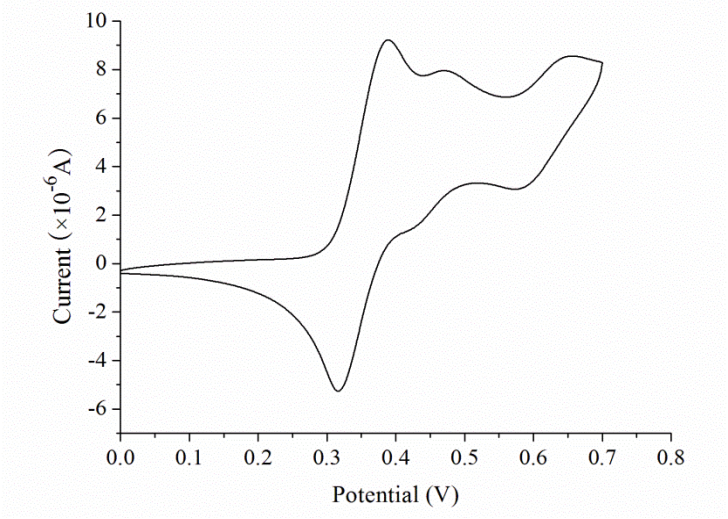

Figure S3 Cyclic voltammetry diagram of compound **TC3T** in anhydrous CH_2Cl_2 with 0.1M Bu_4NBF_4 as electrolyte at a scan rate of 100 $mV \cdot s^{-1}$.

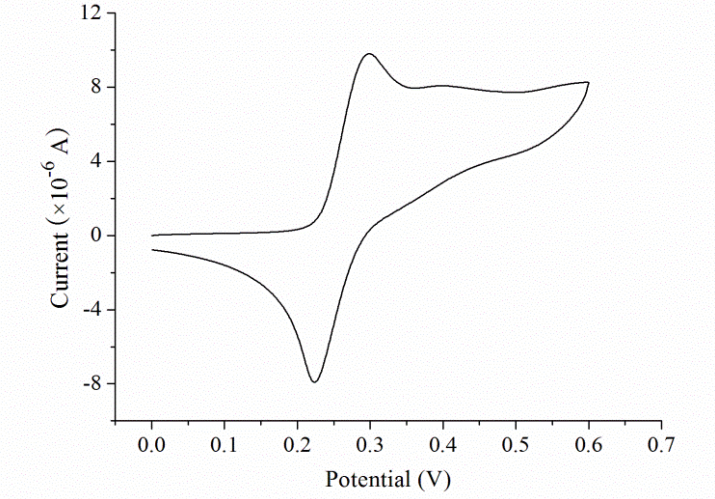

Figure S4 Cyclic voltammetry diagram of compound **PC3P** in anhydrous CH_2Cl_2 with 0.1M Bu_4NBF_4 as electrolyte at a scan rate of 100 $mV \cdot s^{-1}$.

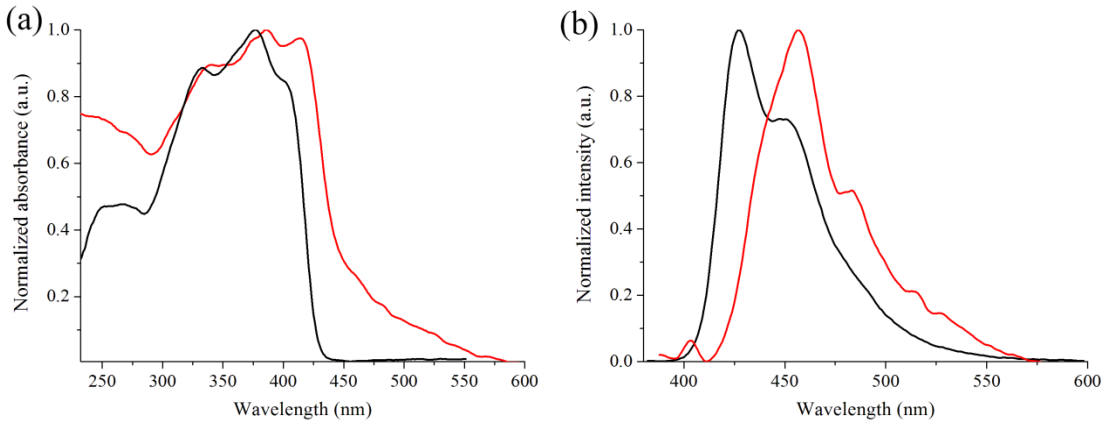

Figure S5 Normalized UV-vis absorbance spectra (a) and Normalized fluorescent emission spectra (b) of **TC3T** in CH_2Cl_2 (black) (1.0×10^{-6} M) and in nanofibers-based films (red).

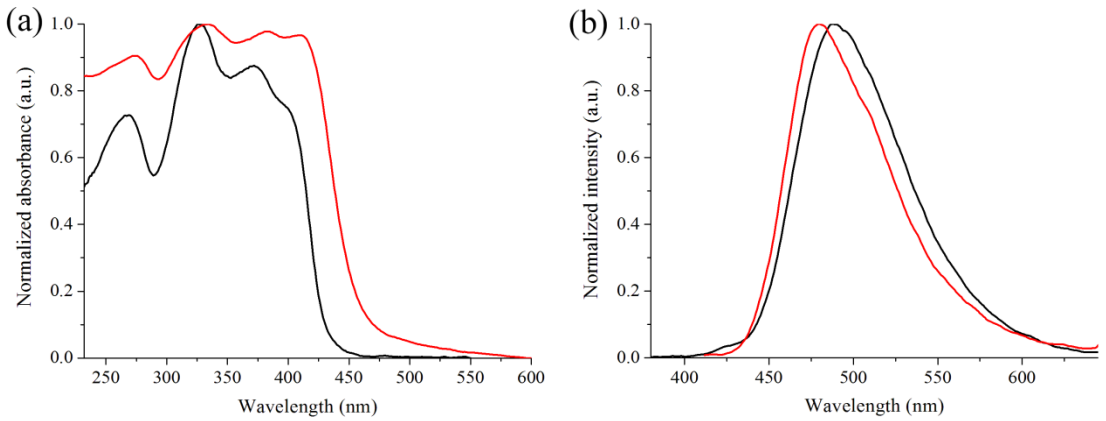

Figure S6 Normalized UV-vis absorbance spectra (a) and Normalized fluorescent emission spectra (b) of **PC3P** in CH_2Cl_2 (black) (1.0×10^{-6} M) and in nanofibers-based films (red).

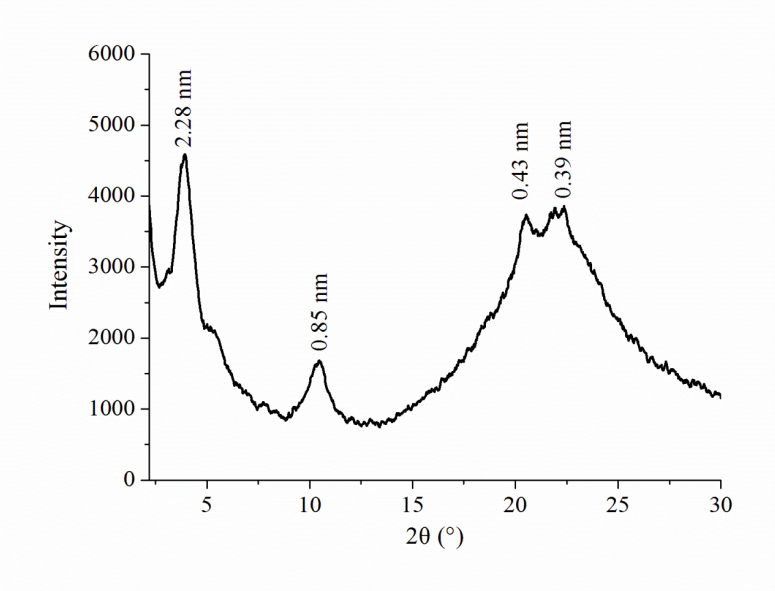

Figure S7 X-ray diffraction pattern of the xerogel **PC3P** obtained from n-Hexane.

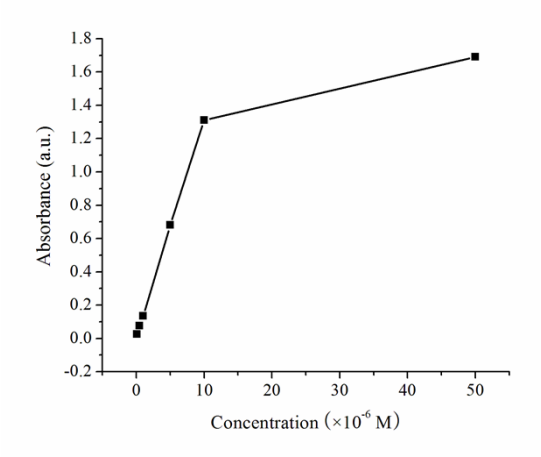

Figure S8 The plot of the absorbance at 326 nm *vers* the concentration of **PC3P** in toluene.

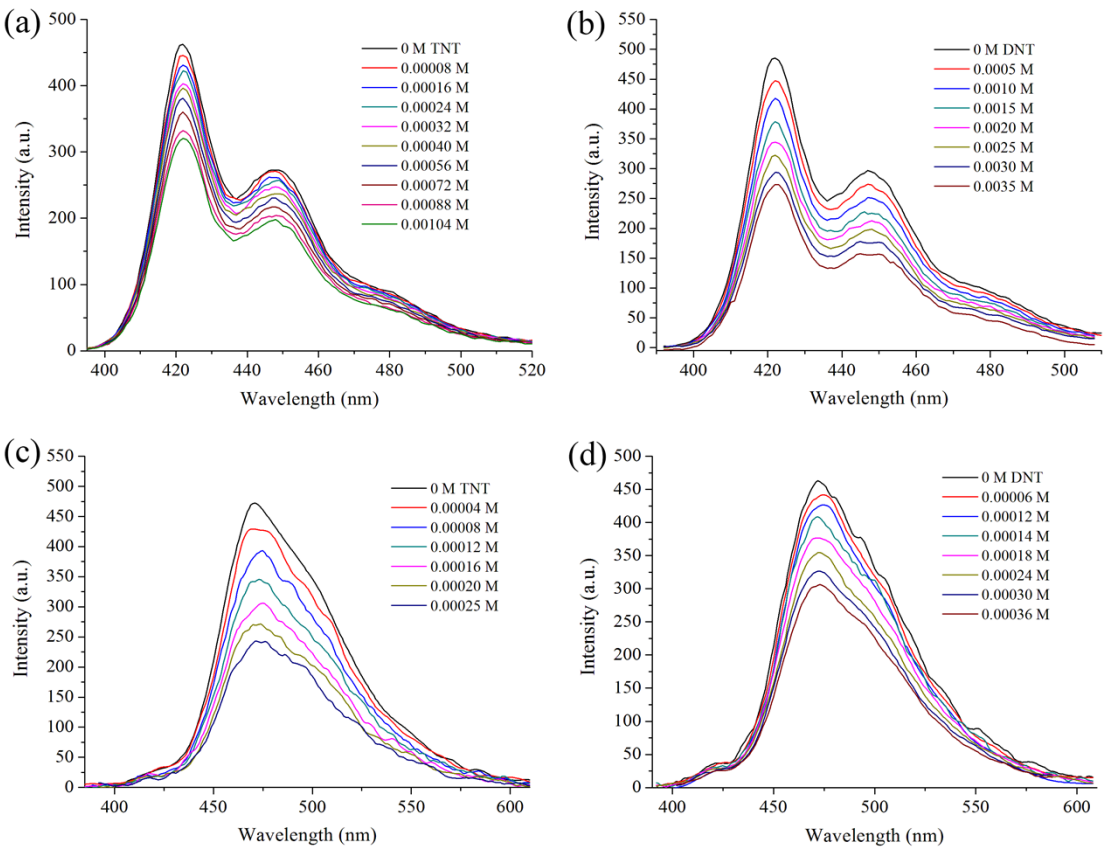

Figure S9 The changes of fluorescent emission spectra of **TC3T** upon addition different amount of TNT (a), DNT (b) and **PC3P** upon addition different amount of TNT (c), DNT (d), respectively, in toluene (1.0×10^{-6} M, λ_{ex} = 330 nm).

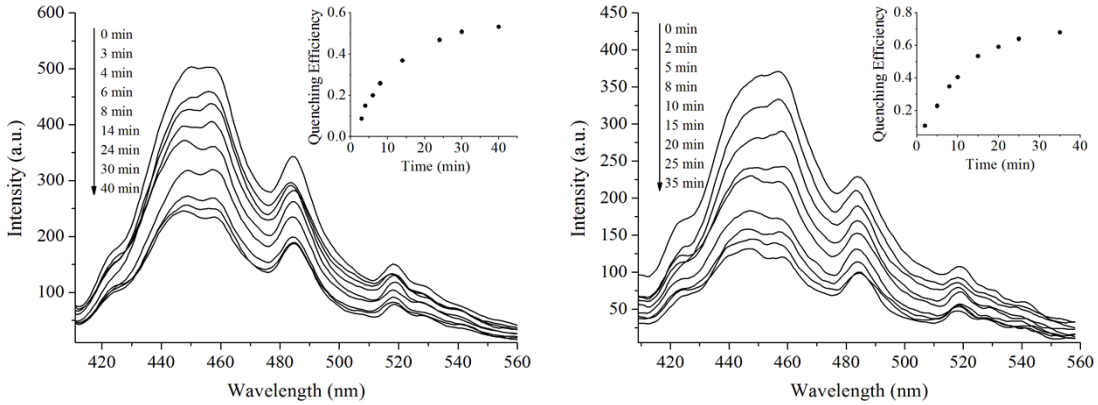

Figure S10 Time-dependent fluorescent emission spectra of nanofibers-based film of **TC3T** (λ_{ex} = 306 nm) upon exposed to the vapors of (a) TNT and (b) DNT. The inset was the fluorescence quenching efficiency against time.

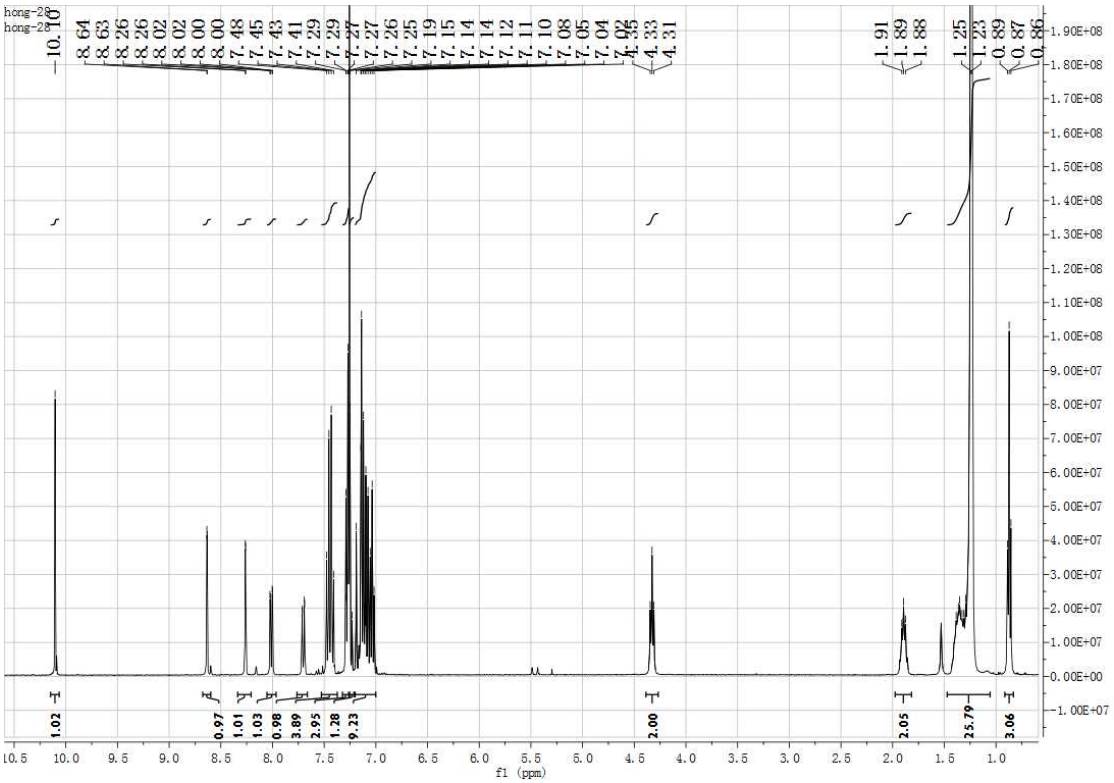

Figure S11 ^{1}H NMR (400 MHz, $CDCl_3$) spectrum of compound **3**.

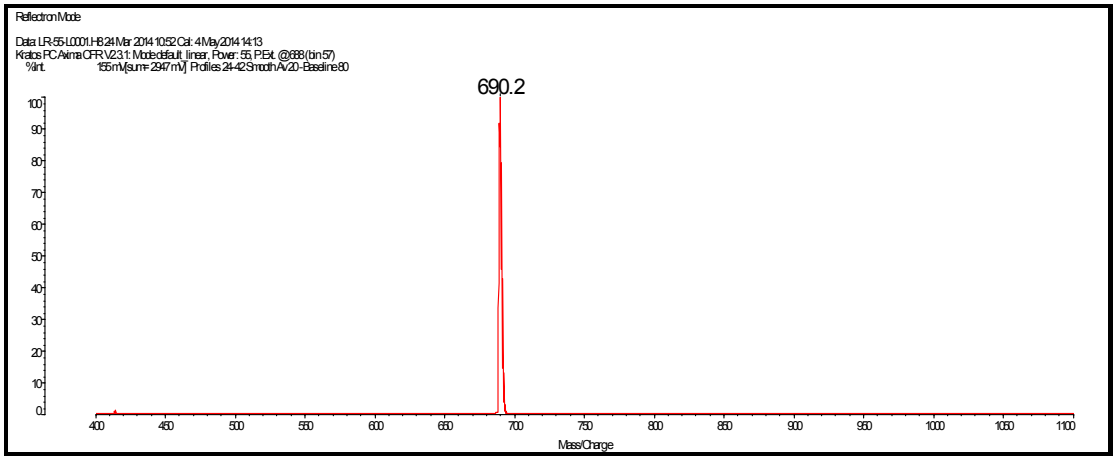

Figure S12 MALDI/TOF MS spectrum of compound **3**.

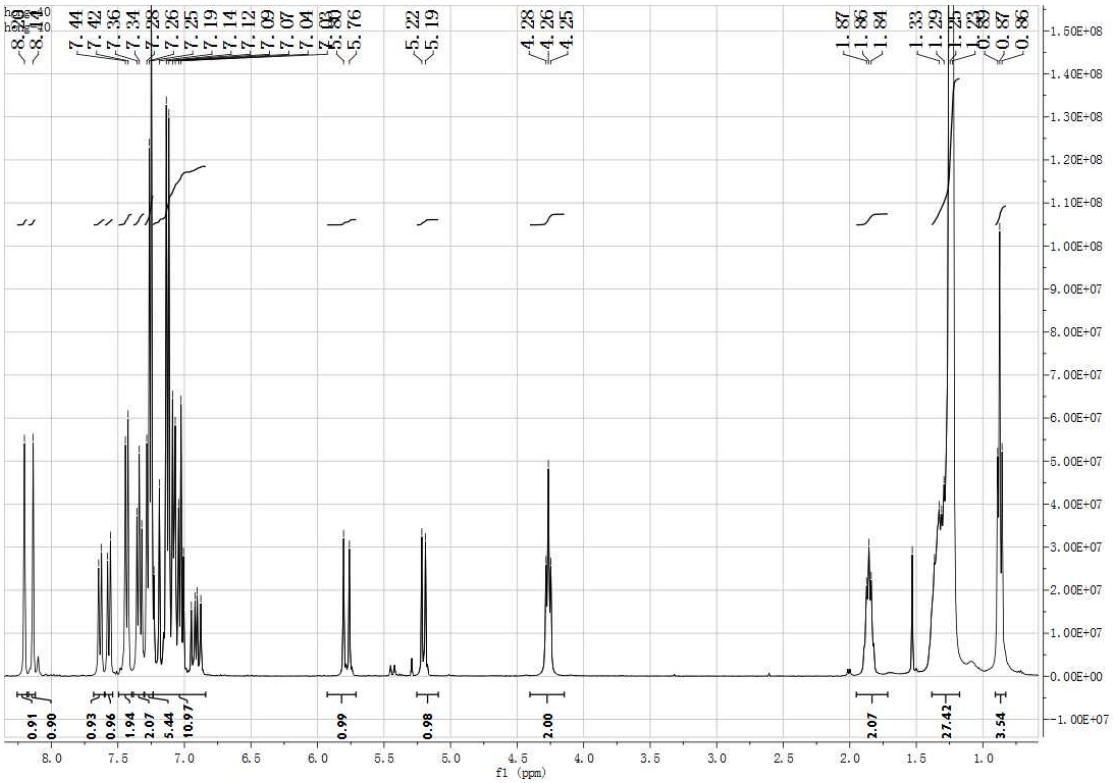

Figure S13 ^{1}H NMR (400 MHz, $CDCl_3$) spectrum of compound **4**.

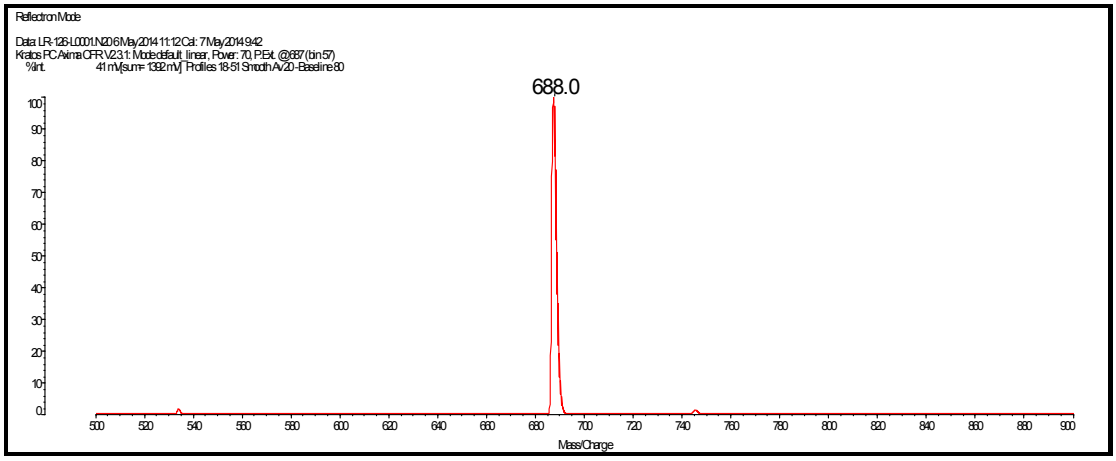

Figure S14 MALDI/TOF MS spectrum of compound **4**.

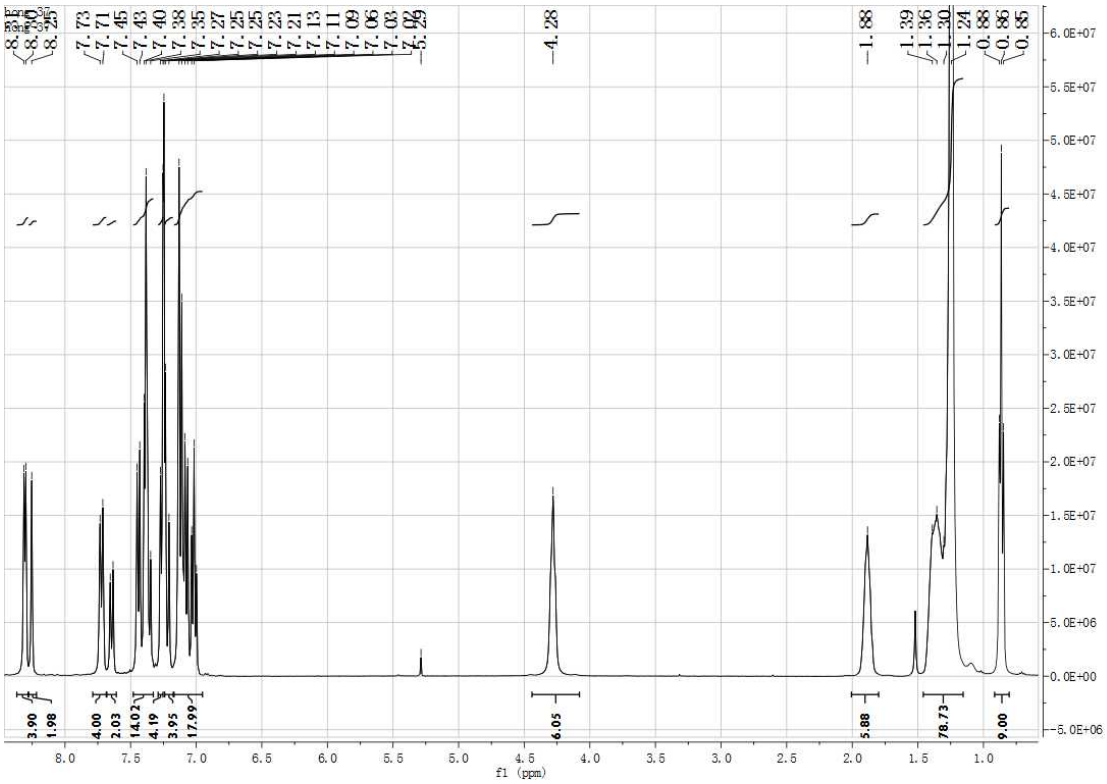

Figure S15 ^{1}H NMR (400 MHz, $CDCl_3$) spectrum of compound **TC3T**.

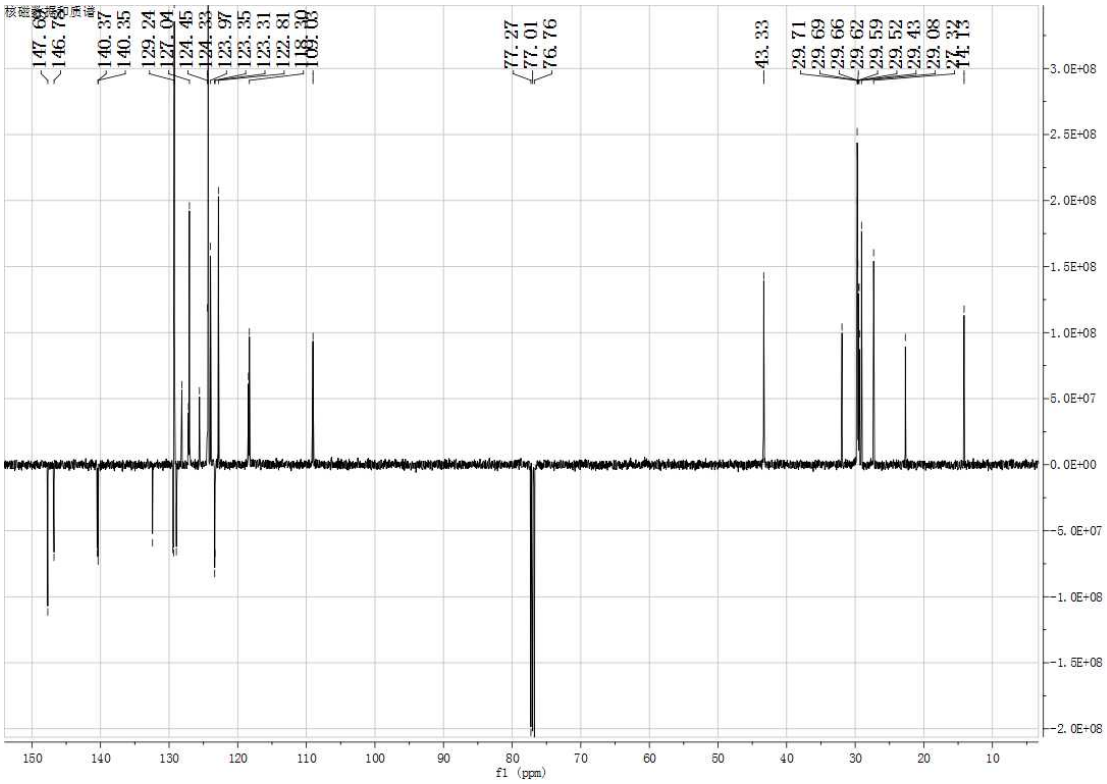

Figure S16 ^{13}C NMR (125 MHz, $CDCl_3$) spectrum of compound **TC3T**.

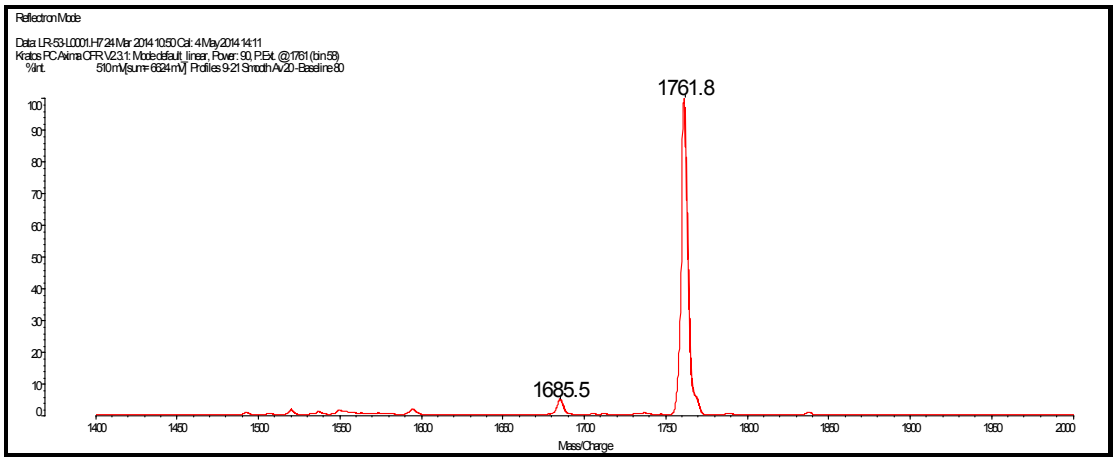

Figure S17 MALDI/TOF MS spectrum of compound **TC3T**.

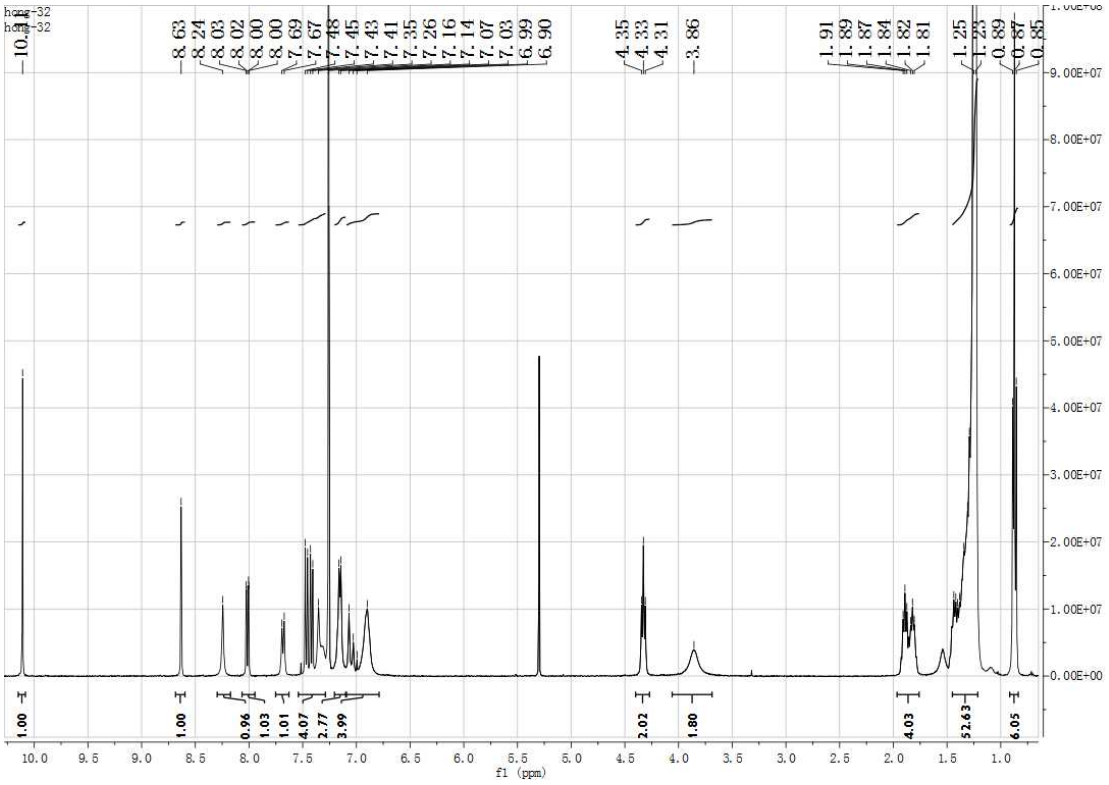

Figure S18 ^{1}H NMR (400 MHz, $CDCl_3$) spectrum of compound **6**.

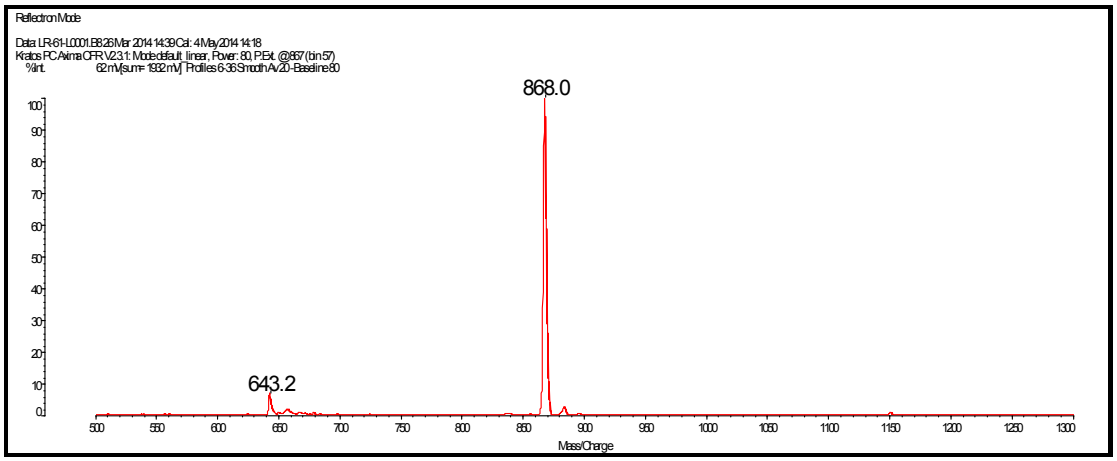

Figure S19 MALDI/TOF MS spectrum of compound **6**.

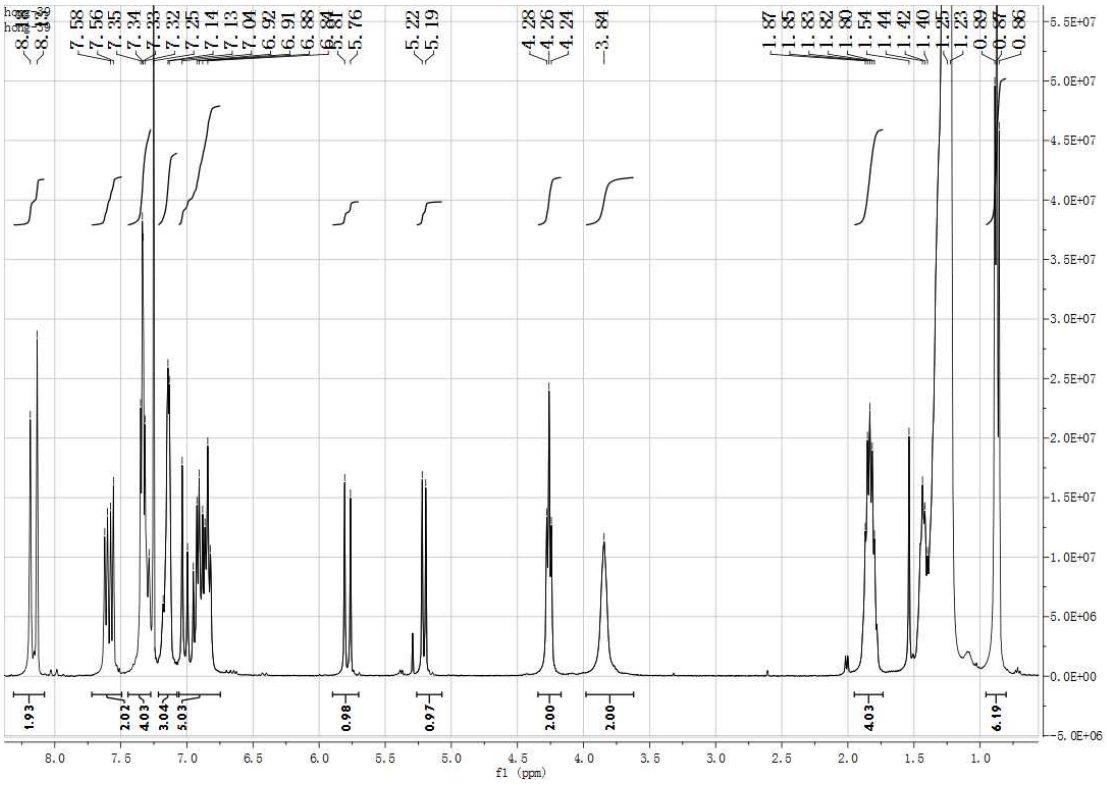

Figure S20 ^{1}H NMR (400 MHz, $CDCl_3$) spectrum of compound **7**.

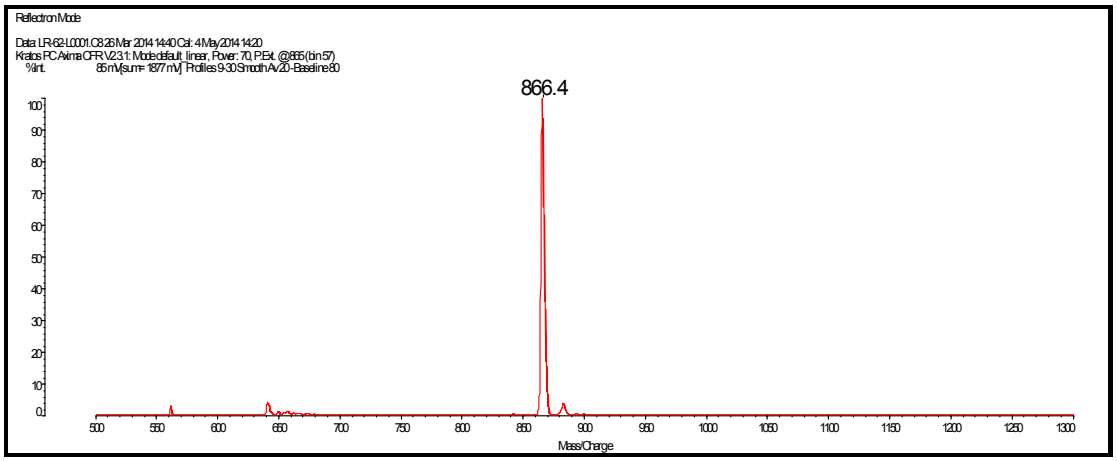

Figure S21 MALDI/TOF MS spectrum of compound **7**.

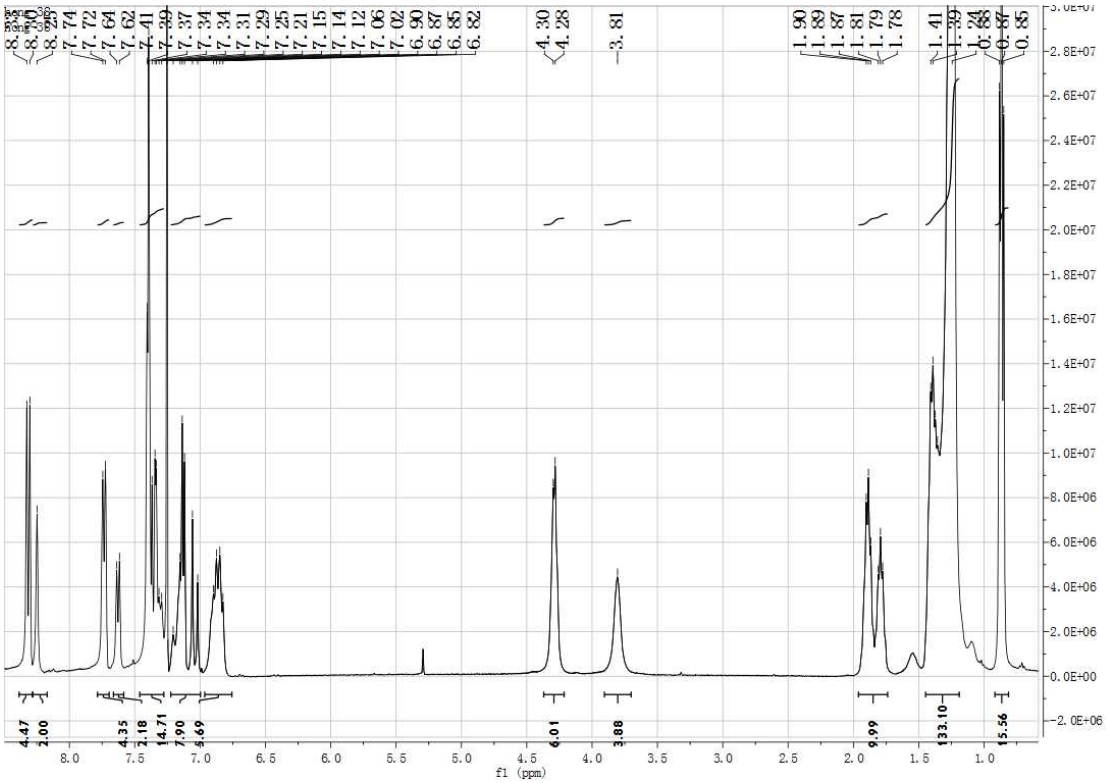

Figure S22 ^{1}H NMR (400 MHz, $CDCl_3$) spectrum of compound **PC3P**.

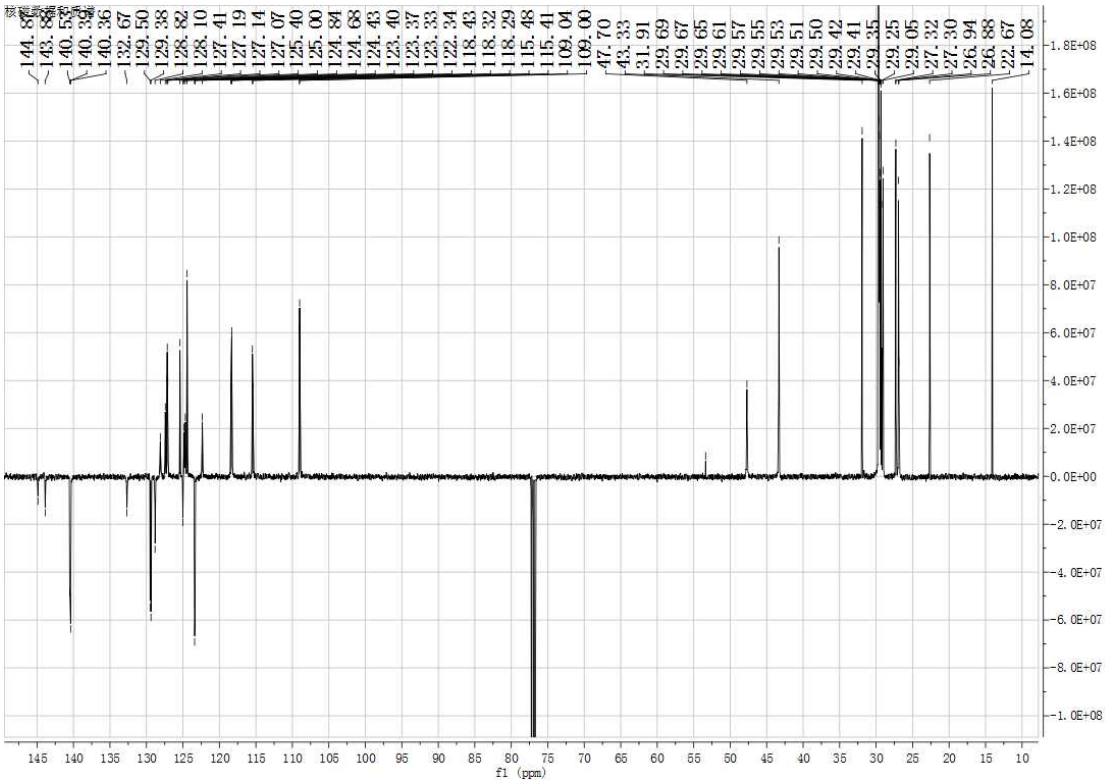

Figure S23 ^{13}C NMR (125 MHz, $CDCl_3$) spectrum of compound **PC3P**.

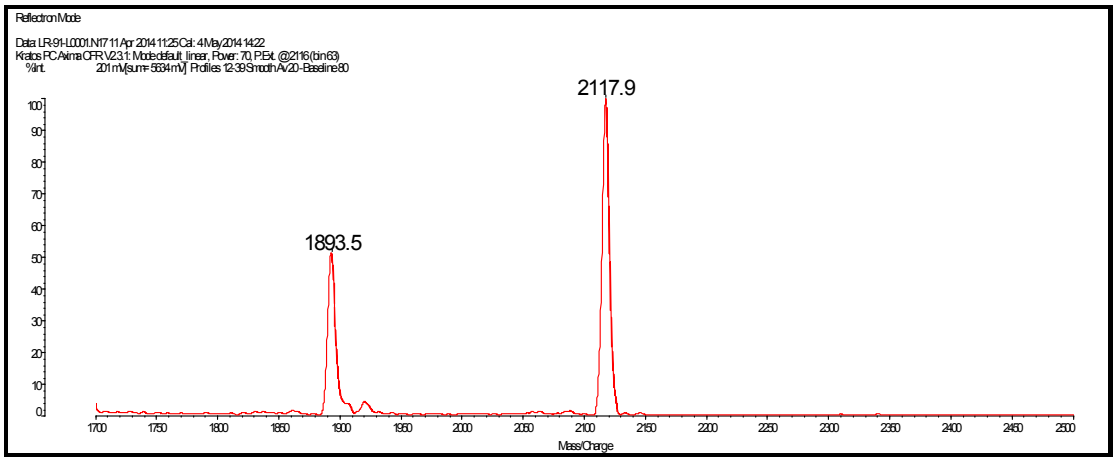

Figure S24 MALDI/TOF MS spectrum of compound **PC3P**.

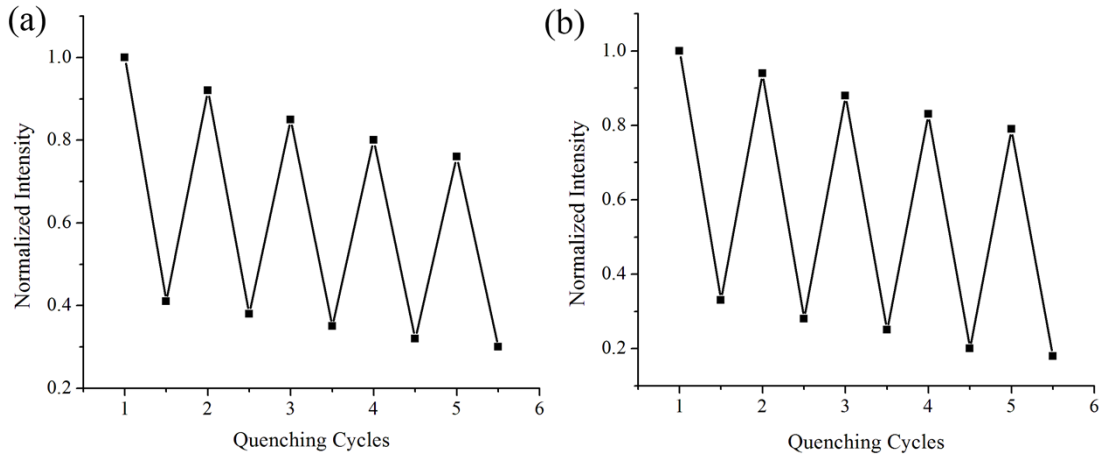

Figure S25 The fluorescence quenching and recovery of **PC3P** in the nanofibers-based film exposed to the saturated vapors of TNT (0.0084 Pa, a) and DNT (0.303 Pa, b) at 40 ºC for 30 min, respectively, followed by blown by dryer for 4 min. The fluorescence intensity at 479 nm was normalized to the initial value before exposed to the saturated vapor of explosives.

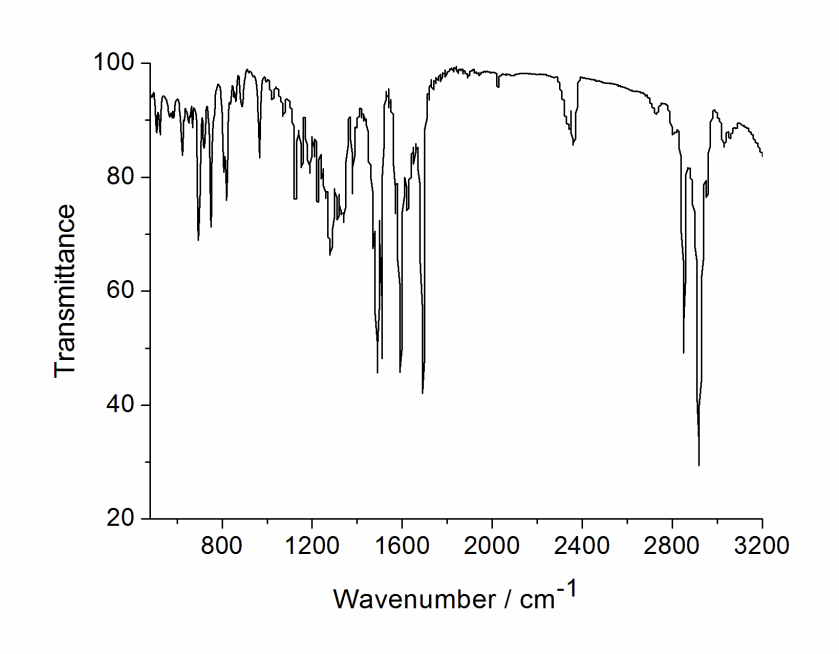

Figure S26 FT-IR spectrum of compound **3**.

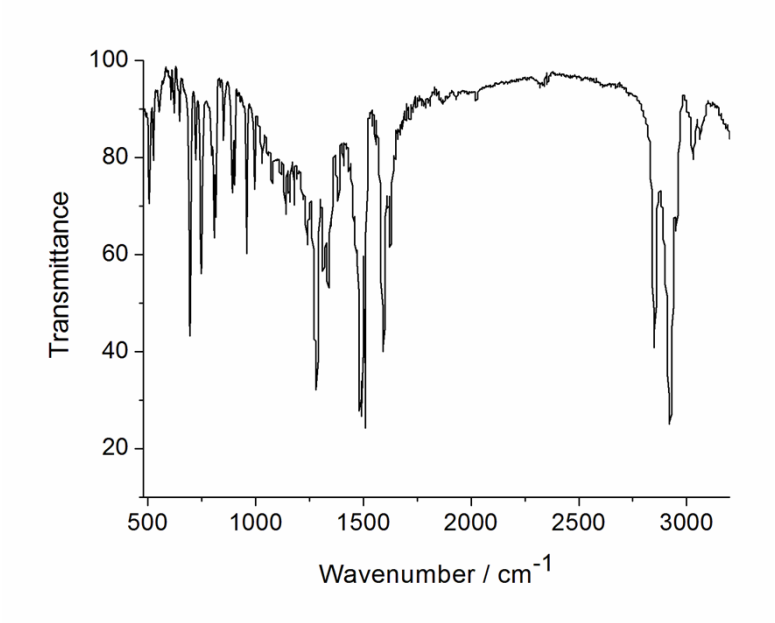

Figure S27 FT-IR spectrum of compound **4**.

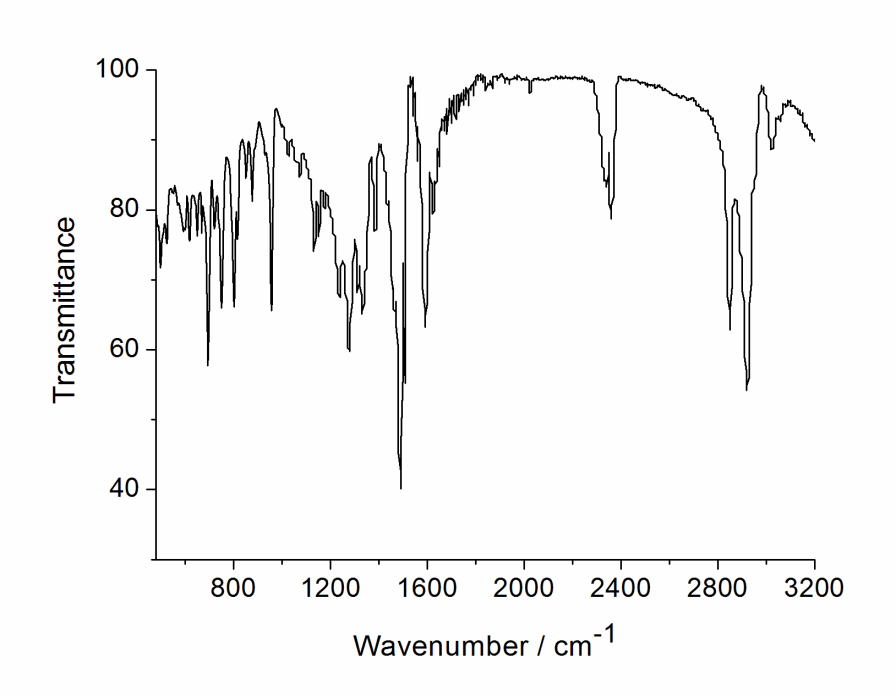

Figure S28 FT-IR spectrum of compound **TC3T**.

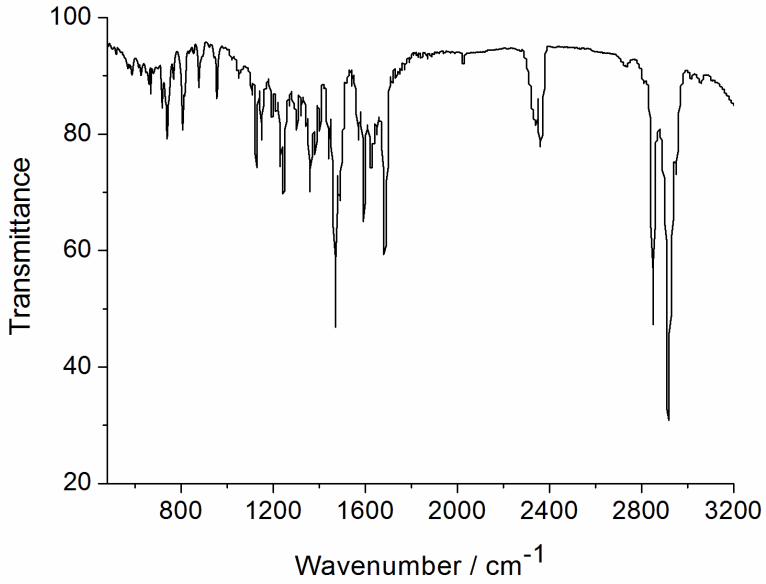

Figure S29 FT-IR spectrum of compound **6**.

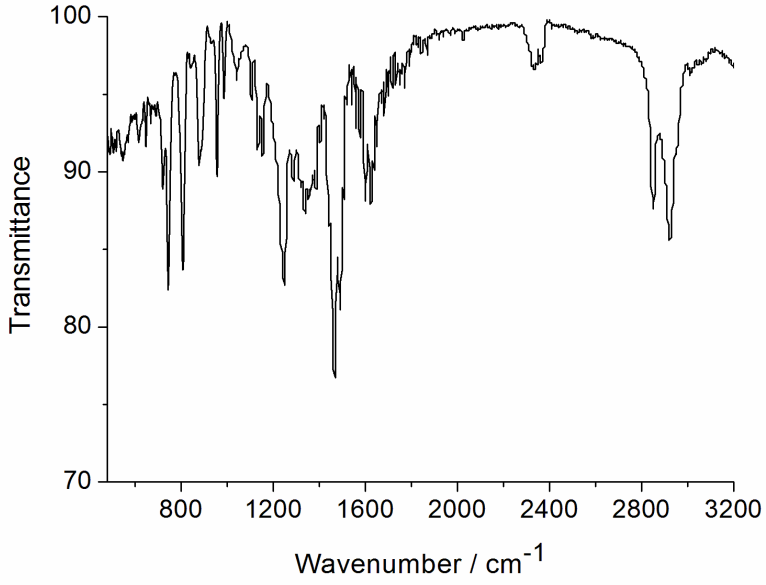

Figure S30 FT-IR spectrum of compound **7**.

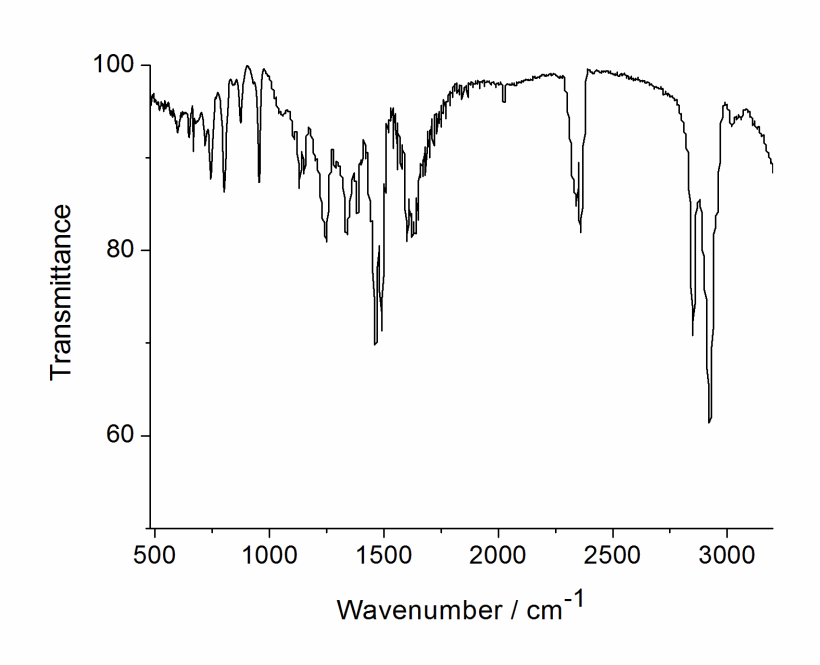

Figure S31 FT-IR spectrum of compound **PC3P**.

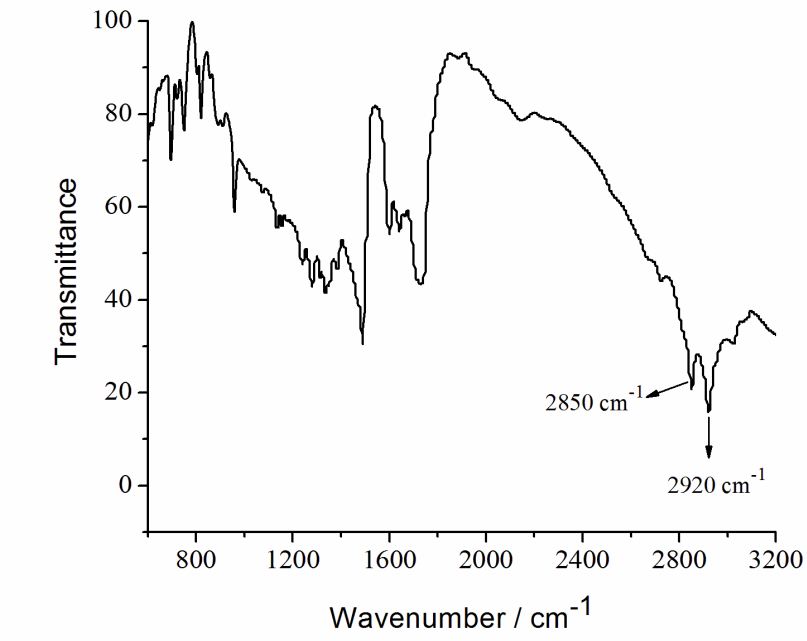

Figure S32 FT-IR spectrum of **TC3T** in xerogel obtained from cyclohexane.